Characteristics of the Ventricular Transient Outward Potassium Current in Genetic Rodent Models of Diabetes

Z. RUSZNÁK, Z. CSERESNYÉS, I. SIPOS, J. MAGYAR, L. KOVÁCS and G. SZÜCS

Department of Physiology, University Medical School of Debrecen, H-4012 Debrecen, P.O. Box 22, Hungary

Abstract. The whole-cell configuration of the patch-clamp technique was employed to measure the transient outward potassium current in enzymatically isolated ventricular cells of spontaneously diabetic rats (BB/Wor) and mice (ob/ob). Healthy littermates (non-diabetic BB rats and lean mice) were used as controls. There was no significant difference between the non-diabetic and diabetic BB rats (Type I diabetes, IDDM) in the amplitude of either the current measured in the absence or the one found in the presence of 4-aminopyridine. The voltage dependence of the activation and steady-state inactivation was also similar in both populations, as no significant difference was observed in the rate of recovery from inactivation of I_{to}. The amplitudes of the total and 4-aminopyridine sensitive currents of lean and obese mice (Type II diabetes, NIDDM) were also similar. The voltage dependences of the activation and of the steady-state inactivation did not differ significantly, either. Our results might indicate certain limitations of the applicability of experiments carried out on genetically diabetic rats if the results are compared to those derived from the healthy littermates as controls.

Key words: BB/Wor rat — Ob/ob mouse — Ventricular cardiomyocytes — Transient outward potassium current — 4-aminopyridine

Introduction

The altered contractility is an early and obligatory finding in diabetic cardiomyopathy (Fein et al. 1980; Tomlinson and et al. 1992). Modifications of different steps in the excitation-contraction coupling might be responsible for the development of this phenomenon. A great body of evidence has accumulated in the recent two decades indicating changes in the intracellular calcium homeostasis and in other

Correspondence to: Dr. Zoltán Rusznák, Department of Physiology, University Medical School of Debrecen, 98 Nagyerdei krt., P.O. Box 22, H-4012, Hungary Phone: (36)-52-316634 FAX: (36)-52-432289 e-Mail: rz@phys.dote.hu

cellular biochemical functions (for a summary see Nagano and Dhalla 1992). Alterations in the contractile activity may originate also from modifications of the surface action potential (Nobe et al. 1990; Tomlinson et al. 1992). The working myocardium of rats and mice has an action potential with no plateau phase in control animals (Watanabe et al. 1983; Schouten 1984; Nobe et al. 1990; Magyar et al. 1992) but a plateau-like prolongation has been reported in diabetic animals by several authors (Fein et al. 1983; Nobe et al. 1990; Magyar et al. 1992).

It is well known that the transient outward potassium current (I_{to}) plays an important role in the repolarization of cardiomyocytes along with other time dependent current components (Josephson et al. 1984; Escande et al. 1985; Benndorf and Nilius 1988; Shibata et al. 1989; Heidbüchel et al. 1990; Apkon and Nerbonne 1991; Nánási et al. 1992). The I_{to} present in cardiac cells has two components: apart from a Ca^{2+}-independent component a Ca^{2+}-dependent one can also be observed which can be inhibited by the application of Co^{2+}. The significance of the transient outward current is prominent in rats and mice, but it contributes to the repolarization of human myocytes as well. We have demonstrated previously that in streptozotocin-(STZ) induced diabetes, the amplitude of the transient outward potassium current decreased and the inactivation of these channels became faster (Magyar et al. 1992). It is generally accepted that STZ-diabetes is a "chemical model" of diabetes (Fein et al. 1981; Schaible et al. 1983; Tomlinson et al. 1992), with the B cells of the Langerhans islets destroyed. This model corresponds to type I diabetes mellitus (Insulin Dependent Diabetes Mellitus, IDDM). However, the question arises whether the damage is restricted to only the B-cells, and whether the apparently diabetes-related changes may be due to direct toxic effects of STZ. Although the fact that modifications observed in STZ-diabetes proved to be partly reversible by insulin treatment (Fein et al. 1981; Schaible et al. 1983; Magyar et al. 1995) argues against the role of toxic side effects, it seemed reasonable to study if the previously reported changes in I_{to} can be noticed in genetically diabetic (BB/Wor) rats, where the side effects of STZ can be excluded. In these animals, IDDM is caused by an autoimmune process (Eisenbarth et al. 1988) and the susceptibility is hereditary (Butler et al. 1988).

To extend our study to type II (Non-Insulin Dependent) diabetes mellitus (NIDDM), a genetic model of this disease was also employed (C57 obese diabetic (ob/ob) mice; Westman 1968; Herberg and Coleman 1977; Bray and York 1979).

Our results indicate that neither the total nor the 4-aminopyridine-sensitive I_{to} density decreased in genetically diabetic animals if compared to the littermates which did not show diabetic syndromes at the time of the experiment. In addition, no differences in the steady-state activation and inactivation were observed. However, the interpretation of these data is complicated because of the nature of the genetic diabetes in the two species studied. Moreover, the presence of various factors which could not be taken into account (insulin treatment, varying glucose

level, etc.) in the present work also made the interpretation of the data difficult. These uncertainties might be overcome in the future by more specifically designed experiments.

Materials and Methods

Animals, nomenclature

BB/Wor rats were purchased from Mollegaard Breeding Centre Ltd. (Ejby, Denmark), the BB/Wor/Mol-BB colony, and one further generation was bred in our vivarium. Hyperglycemia developed in 36 rats before the 12^{th} week of their lifetime (corresponding to 92% incidence). Without proper insulin treatment, the diabetic rats fell into hyperglycemic coma and died within 24–48 hours, hence these animals had to be treated with insulin (0.5–5 IU/day/animal, Ultralente, Novo Industri AS, Copenhagen). The daily dosage was adjusted on the basis of the blood glucose levels (checked twice a week). Whenever the term "diabetic rat" is used herein, it always refers to animals in which diabetes developed and was controlled by insulin. Diabetes persisted and insulin treatment was administered for 4–10 weeks. The age of the rats used for the present work was 12–24 weeks; their blood glucose levels and weights varied between 18–22 mmol/l and 170–350 g, respectively, during the period of the experiment. Animals served as controls in this series of experiments which did not show symptoms of diabetes until week 18 of the lifetime. The age of these rats was 18–24 weeks, their blood glucose levels and weights varied between 5–7 mmol/l and 290–405 g, respectively ($n = 3$) immediately prior to the experiment.

Genetically diabetic mice were bred in our vivarium. In these experiments, the lean animals were used as controls, referred to as "controls" or "lean mice". (Their homozygous +/+ or heterozygous ob/+ genetic status was not taken into account). The diabetic homozygous ob/ob animals are referred to as "obese mice" throughout. All animals used (7 obese and 10 control mice) were 6–7 month-old, their body weights varied between 50–60 g and 20–25 g, respectively. The obese mice were in a moderate hyperglycemic state in comparison with the lean ones (serum glucose level ranged between 9 and 14 mmol/l in obese, and from 5 to 9 mmol/l in control animals, measured at the time of the experiment). These values are in good agreement with previous findings (e.g. Lord and Atkins 1985).

Cell isolation and incubation

Ventricular cardiomyocytes were isolated using procedures described previously (Magyar et al. 1992). The animals were killed with a blow on the neck, the hearts were removed and perfused on a Langendorff column in three steps. The solutions were oxygenated continuously, and their temperature was kept at +37 °C. The chemicals were purchased from REANAL (Budapest, Hungary) and from SIGMA

(St. Louis, Mo, USA). In the first step, Tyrode's solution with reduced Ca^{2+} content (in mmol/l: NaCl, 150.0; KCl, 5.4; $MgCl_2$, 0.5; $CaCl_2$, 1.0; HEPES, 5.0; glucose, 1.1; pH set to 7.2 using NaOH) was applied for 2–3 minutes in order to wash out blood of the coronary vessels. In the second step, nominally Ca^{2+}-free Tyrode's solution was perfused for 5 min, while in the last step 180 μmol/l Ca^{2+} and 5–8 mg/40 ml collagenase (Type I, SIGMA) containing Tyrode's solution was used for 20–35 min (usually longer digestion time was needed in rats than in mice). The portions of cell suspension were separated and stored in an incubating solution (in mmol/l: KCl, 85.0; KH_2PO_4, 30.0; $MgCl_2$, 3.0; glucose, 10.0; K-glutamate, 16.0; EGTA, 0.5; $KHCO_3$, 3.0; pyruvic acid, 5.0; HEPES, 10.0; taurine, 20.0; pH adjusted to 7.4 with KOH) at +5 °C at least for one hour.

The measurements were carried out at room temperature in a measuring chamber placed on the stage of an OLYMPUS CK-2 inverted microscope. The current measurements started in 2.0 mmol/l Ca^{2+}, 20 μmol/l TTX and 3.0 mmol/l Co^{2+} containing Tyrode's solution. In some experiments, 3.0 mmol/l 4-aminopyridine (4-AP) was applied.

Voltage clamp experiments

To study the ion currents, the whole-cell clamp configuration of the patch clamp technique was employed (Hamill et al. 1981). The microelectrodes were made of thin walled Pyrex glass capillaries (Clark Electromedical Instruments, UK), and had a 3–5 MΩ resistance when filled with the internal solution (in mmol/l: K-aspartate, 130.0; KCl, 20.0; KH_2PO_4, 1.0; $MgCl_2$, 1.0; EGTA, 5.0; Na_2-ATP, 3.0; HEPES, 5.0; pH set to 7.3 with KOH). Currents were recorded by either an AXOPATCH-1D or AXOPATCH-200 amplifier (Axon Instruments, Foster City, CA). Pulse control and data acquisition were performed by IBM PCs equipped with a Labmaster TM40 12 bit AD/DA converter (Scientific Solutions, Foster City, CA), and using the pCLAMP 5.6 software (Axon Instruments, Foster City, CA). The sampling rate varied between 2.8 and 33 kHz.

Data analysis, statistics

Membrane capacitance of the cells was determined by symmetrical 5 mV steps from the holding potential of −85 mV. The leakage current was determined by hyperpolarizing pulses of 5 mV, and the linearly extrapolated values were subtracted from the current traces at the start of the analysis. The current amplitudes were measured as deviation from the zero current level except when determining the size of the inactivating component (see Results).

The fitting procedures were based on a χ^2 minimizing Levenberg-Marquardt algorithm (Schreiner et al. 1985). In the cases of the steady-state inactivation and the rate of recovery from inactivation, the fitted parameter values were grouped into a histogram. The bin width of this histogram was constant, and its bar height

represented the total number of points found in the given interval, divided by the total number of the points and by the bin width. This histogram, which was similar to Gaussian distribution, was fitted by the probability density function of the Gaussian distribution:

$$f(x) = ((2\pi\sigma^2)^{-0.5} \cdot \exp(-(x-m)^2/(2\sigma^2)) \tag{1}$$

where m is the mean value, and σ is the standard deviation.

All data in this paper are given as mean ± SD. The error bars in the Figures represent SD unless indicated otherwise. Student's paired and unpaired t-tests were used for statistical analysis.

The steady-state inactivation of the I_{to} was determined by a pulse protocol where a constant, 700 ms long test pulse with an amplitude of +50 mV was preceded by a prepulse of 700 ms duration. The prepulse potential varied between −100 and 0 mV with 10 mV steps. The amplitude of the I_{to}, which was evoked by the test pulse, was determined as the difference between the peak and the current measured at the end of the 500 ms long depolarizing stimulus. These amplitudes were normalised to the maximal value measured with the −100 mV prepulse. The non-inactivated ratios calculated in this way (R_{ni}) were averaged and plotted as a function of the membrane potential during the prepulse. The data points belonging to the individual cells were fitted by the equation

$$R_{ni} = 1/(1 + \exp((V_p - V_{50})/s)) \tag{2}$$

where V_p and V_{50} are the prepulse potential and the half-inactivation membrane potential, respectively, and s is the slope factor.

The rate of recovery from inactivation of I_{to} was determined by a double pulse protocol, too. Both pulses had the same parameters (depolarization of +50 mV with a duration of 700 ms from a holding potential of −85 mV), whereas the time interval between them changed from 1 to 400 ms. The size of the peak current was measured as described before. The peak value during the second pulse was divided by that belonging to the first pulse, and the reactivated ratios (R_{react}) were averaged. To describe the kinetic behavior of the recovery, data of the individual myocytes were fitted to the equation

$$R_{react} = R_{max}[1 - \exp(-t/\tau)] \tag{3}$$

where R_{max} is the maximal reactivated ratio in a given cell, t is the interpulse interval and τ is the time constant of the recovery.

Results

Characterization of the I_{to} in BB/Wor rats

Characteristic features of the I_{to} in non-diabetic and diabetic BB rats are illustrated in parts *A* and *B* of Fig. 1, respectively. The values were normalised to the whole-cell capacitance (the cell capacitance was 164 ± 37 pF in non-diabetic rats, and 202 ± 34 pF in diabetic animals). The currents were evoked by test pulses of 500

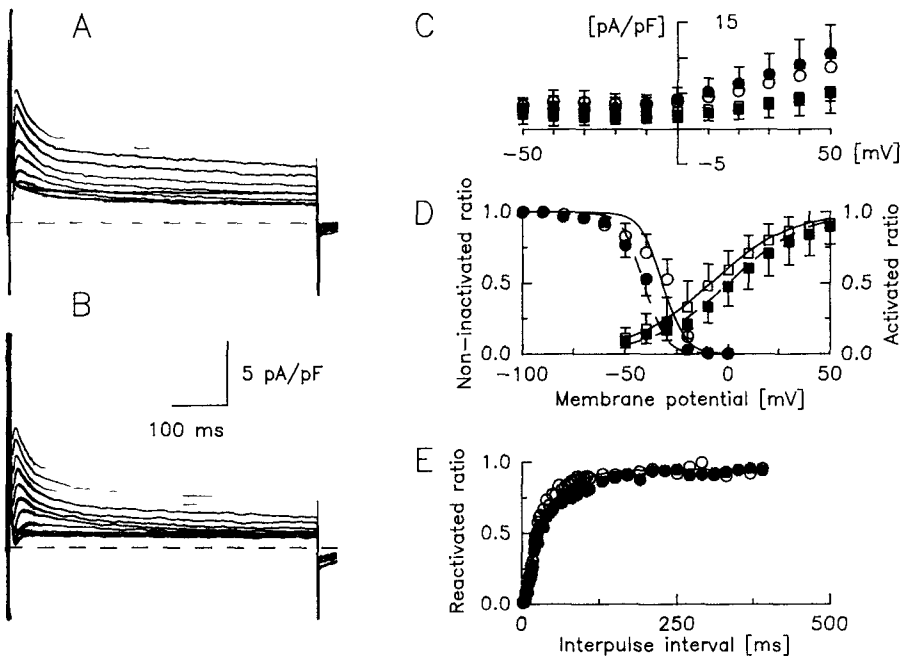

Figure 1. Current traces obtained on depolarization from ventricular cardiomyocytes of a non-diabetic (*A*) and a diabetic BB rat (*B*). Broken lines indicate zero current level. *C*: Current-voltage relationships of the peak (circles) current and the current measured at 500 ms (squares). Data points represent the average of 19 individual values in the cases of controls (open symbols) and 33 values in the cases of diabetic BB rats (filled symbols). There is no significant difference between non-diabetic and diabetic animals. *D*: Membrane potential dependence of activation and steady-state inactivation. Activation was determined in 19 cells in control (open squares) and in 33 myocytes in diabetic rats (filled squares), steady-state inactivation was calculated in 5 cells from non-diabetic (open circles) and in 9 cardiomyocytes from diabetic animals (filled circles). The continuous (control) and the broken lines (diabetes) were constructed using Eq. (2). The symbols represent mean ± SE. *E*: Time course of the recovery from inactivation of I_{to} (at −85 mV). Data points represent 3 control cells (open circles) and 9 diabetic myocytes (filled circles). The continuous (control) and the broken lines (diabetes) were constructed from Eq. (3). The error bars are omitted for proper visibility.

ms duration from a holding potential of −85 mV to voltages between −50 and +50 mV in 10 mV increments. The test pulse was always preceded by a prepulse with a duration and amplitude of 7 ms and −20 mV, respectively, in order to inactivate the TTX-insensitive Na^+ current. The comparison between the *I–V* curves presented in part *C* of Fig. 1 proves that neither the peak current of the I_{to} nor the current measured at 500 ms of diabetic BB rats differ significantly from those found in control animals.

The steady-state inactivation of the I_{to} (Fig. 1*D*) was determined by a technique described in the Material and Methods section. V_{50} was -32 ± 7 mV for non-diabetic and -41 ± 10 mV for diabetic cells, the shift is statistically not significant. The slope factor was not significantly different either (5.3 ± 0.9 mV for non-diabetic and 5.1 ± 0.9 mV for diabetic cells).

When deriving the voltage dependence of the activation of the I_{to}, first the conductances ($g(V)$) were calculated for the individual cells. The peak values of the I_{to} were divided by the driving force (the difference between the actual membrane potential and the holding potential ($V_p - V_H$; Tytgat et al. 1990). The obtained data were fitted to the term on the right side of Eq. (2). The value of the slope factor was -19 ± 7 mV for diabetic rats and -20 ± 9 mV for non-diabetic animals, the difference was not significant.

Values of g_{max} were 55 ± 17 pS/pF and 49 ± 22 pS/pF, and the half-activation voltages were -8 ± 16 mV and -1 ± 11 mV for non-diabetic and diabetic rats, respectively. Neither of the above differences was statistically significant.

The parameters obtained in order to compare the recovery from inactivation of the I_{to} were not statistically different in the two groups of animals: the R_{max} values were 0.95 ± 0.05 and 0.93 ± 0.07, and the time constants were 38 ± 7 ms and 45 ± 15 ms for the non-diabetic and diabetic myocytes, respectively (Fig. 1*E*).

Characterization of the I_{to} in cells from lean and obese mice

Analysis of the I_{to} in murine cells was carried out using the same experimental protocols and the same evaluation methods as described for the BB rats. The results of this analysis are presented in Fig. 2. Parts *A* and *B* show the current families in cells of a lean and an obese mouse, respectively. (The mean cell capacitance was 134 ± 55 pF for the lean, while 98 ± 37 pF for ob/ob mice.) When constructing the *I–V* relationships (part *C*), the end-pulse current (measured at 500 ms) was also determined. No difference was found between the lean and the obese mice either in the amplitude of the I_{to} or in the current measured at 500 ms.

Part *D* of Fig. 2 illustrates the membrane potential dependence of activation and steady-state inactivation of I_{to}. The analysis of the data did not establish any significant differences between the two groups of animals. In the case of the steady-state inactivation, the half-inactivation voltages (obtained by Eq. (2)) were -45 ± 5 mV and -42 ± 5 mV, and the slope factors were 7.6 ± 0.8 mV and 8 ± 2 mV for

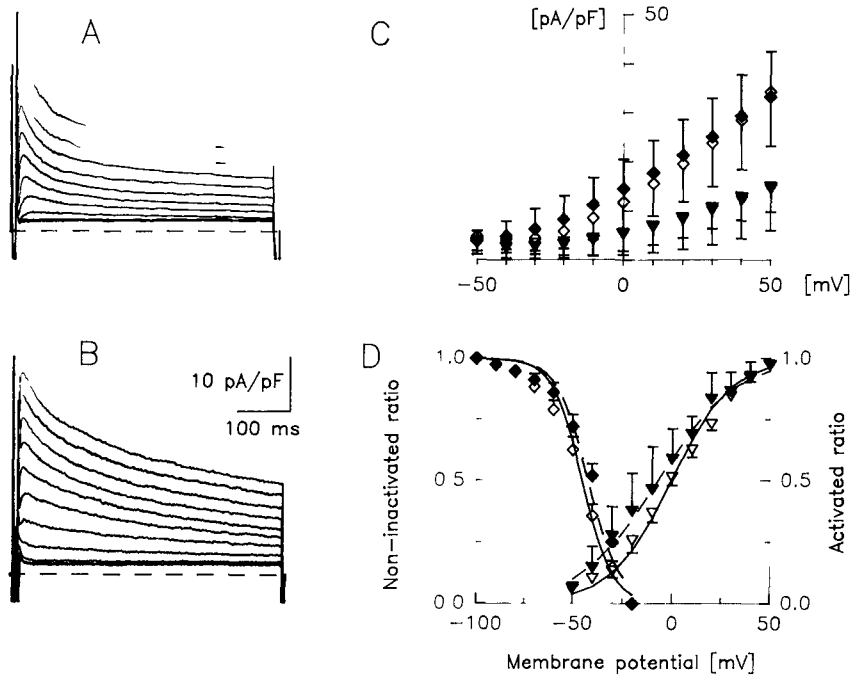

Figure 2. Current traces obtained on depolarization from ventricular cardiomyocytes of a lean (*A*) and an obese mouse (*B*). Broken lines show zero current level. *C*: Current-voltage relationships of the peak (diamonds) current and the currents measured at 500 ms (triangles). The data points provide the average of 24 control cells (open symbols) and 13 myocytes from obese animals (filled symbols). There is no significant difference between lean and obese animals. *D*: Membrane potential dependence of activation and steady-state inactivation. Activation (triangles) and steady-state inactivation (diamonds) were determined in 24 cells from lean (open symbols) and in 13 myocytes from obese mice (filled symbols). The continuous (control) and the broken lines (diabetes) were constructed using Eq. (2). The symbols represent mean ± SE.

lean and obese mice, respectively. The activation was calculated as described in the Fig. 1. The maximum conductance was 136 ± 33 pS/pF for lean and 152 ± 42 pS/pF for obese mice. These values are considerably larger than the corresponding ones obtained for BB rats. The half-activation voltages were 1 ± 6 mV and −6 ± 8 mV, the absolute values of the slope factors were 15 ± 5 mV and 20 ± 7 mV for lean and obese animals, respectively.

Separation of the 4-AP-sensitive current

The data described in the previous sections indicate that there is no appreciable change in the magnitude of the I_{to} contrary to the considerable decrease found in rats, where diabetes was initiated by STZ treatment. In this series of experiments, the pharmacological analysis was limited to the separation of the 4-AP-sensitive

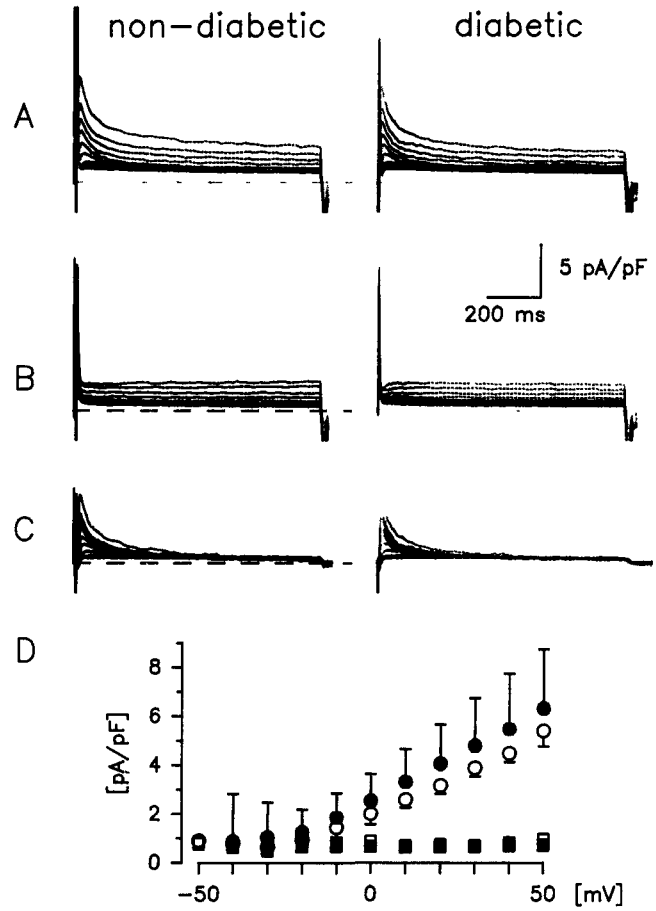

Figure 3. Separation of the 4-AP-sensitive current components in BB rats, in the case of cardiomyocyte from a a non-diabetic and a diabetic animal. The current traces were obtained using the pulse protocol described in the legend to Fig. 1*A*, in Tyrode's solution (*A*), and between min. 10 and 13 of 3 mmol/l 4-AP application (*B*). The lower families represent the differences between the above two families and, consequently, the 4-AP-sensitive component (*C*). The broken line indicates zero current level in each case. *D*: Current-voltage relationships of the 4-AP-sensitive (circles) and 4-AP-insensitive (squares) currents in cells from non-diabetic (open symbols, $n = 5$) and diabetic (filled symbols, $n = 14$) BB rats. There is no statistically significant difference between the two groups of animals.

current, which emerged as a major target of the STZ-related modifications (Magyar et al. 1992).

During the separation, first a current family in the control extracellular solution was recorded. Following this, 3 mmol/l 4-AP was added to the bath, and the same pulse protocol was applied again. The traces recorded in the presence of 4-AP were then subtracted from those obtained in Tyrode's solution, and the difference curves are termed "4-AP-sensitive current".

This procedure is illustrated in parts *A* and *B* of Fig. 3 in the cases of car-

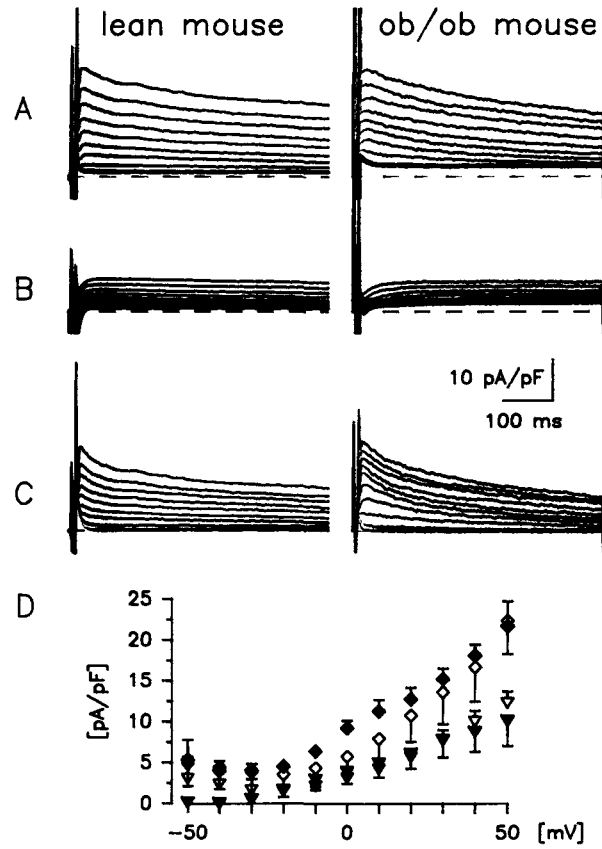

Figure 4. Separation of the 4-aminopyridine current components in cells from a lean and an obese mouse. The total (*A*), 4-AP-insensitive (*B*) and 4-AP-sensitive (*C*) traces were constructed as described in the legend of Fig. 3. *D*: Current-voltage relationships of the 4-AP-sensitive (diamonds) and 4-AP-insensitive (triangles) currents in cells from lean (open symbols, $n = 7$) and obese (filled symbols, $n = 4$) mice. There is no statistically significant difference between the two groups of animals.

diomyocytes of a non-diabetic and a diabetic BB rat, respectively. The transient component proved to be entirely 4-AP-sensitive, leaving only a small steady-state component. Moreover, part C of the Figure shows that there is no difference between the non-diabetic and the diabetic rats regarding the size of the 4-AP-sensitive components.

This procedure was carried out in mice as well, repeating step by step the method described for rats. Fig. 4 presents the total, the 4-AP-insensitive, and the 4-AP-sensitive traces (from top to bottom). The transient component proved to be entirely 4-AP-sensitive in this case, too. Unlike in rats, however, the slowly inactivating current was partly inhibited by the channel blocker.

Discussion

Diabetes in rats – IDDM

The electrophysiological changes in type I diabetes (IDDM) evoked in Wistar rats by application of STZ were characterized by a decreased amplitude of I_{to} as well as by an increased inactivation speed of the surviving conductance (Magyar et al. 1992). These changes seemed to be absent when comparing the values of these parameters measured in diabetic BB rats to those found in non-diabetic animals of the same strain. This finding is similar to the report of Rodrigues et al. (1989) who did not establish any significant difference in the Ca^{2+} transport in the sarcoplasmic reticulum between low-dose insulin treated diabetic BB rats and their non-diabetic littermates. When interpreting this finding, however, two main issues have to be pointed out.

First, it is uncertain to which extent the non-diabetic rats can be considered as "healthy" controls. The BB/Wor model was developed from Wistar rats by a mutation (Chappel and Chappel 1983), and the incidence of the IDDM in these animals is rather high due to an autoimmune process destructing the B cells in the Langerhans islets (Eisenbarth et al. 1988). The appearance of the disease is typical at the age of 8–12 weeks (Hansen 1989), and it is characterised by severe hyperglycemia and loss of body weight (Herberg and Coleman 1977). If the symptoms are absent after this age, the animal is used as control, but it still can be a potential diabetic one, and it is impossible to check whether manifest diabetes would have occurred some days after the experiment.

It is important to point out that when the size of I_{to} found in BB rats was compared to that measured in Wistar rats, values for both the diabetic and the non-diabetic animals were very similar to those obtained for STZ-diabetic animals (Magyar et al. 1992). This accord may be incidental, but it may also indicate that alterations similar to those caused by STZ are present in the BB rats independently of whether clinical symptoms of IDDM have or have not developed.

The second problem with respect to the comparison is the insulin treatment

of the diabetic BB rats. The STZ-diabetic rats survive for months without any intervention, probably due to incomplete destruction of the B cells by the STZ doses applied (Rerup 1970). The diabetic BB rats, however, fall into hyperglycemic coma and are lost unless insulin is regularly administered. It is known that insulin is capable of normalising several altered parameters, including the decreased density of I_{to}, in STZ diabetic rats (Fein et al. 1981; Schaible et al. 1983; Magyar et al. 1995). The lack of difference between the two groups of BB rats, therefore, may be due to the insulin treatment itself.

The I_{to} changes are likely a result of a membrane disorder which is typical of IDDM. Such a generalized membrane disfunction is supported by the fact that even non-diabetic BB rats may suffer from other diseases like hypothyreosis (Rajatanavin et al. 1991). It is worth noting that thyroid disorders are also accompanied by changes in I_{to} (Shimoni et al. 1992), in cardiac β-receptor density and in contractile parameters (Tomlinson et al. 1992).

Another indication of a non-specific membrane disfunction may be the finding that the plasma lipid levels are significantly higher both in non-diabetic and in diabetic BB rats than in the Wistar rats (Rodrigues et al. 1989). The increased tissue lipid levels may modify the interaction between the hydrophobic regions of the membrane proteins and the lipids (Katz and Messineo 1981), influencing both the receptor and the channel functions. A survey in STZ-diabetic rats oricuted towards these aspects could be informative.

Although the alterations in cardiac electrophysiology are not the cardinal symptoms in diabetes, the results presented in this paper provide some arguments for the interpretation of models of diabetes. As an objection against the use of the chemical models, the possible toxic side effect(s) of the drugs can be mentioned. The decreased amplitude of the transient outward potassium current in STZ-diabetic rats is a finding not seen in the genetic models. Thus, this difference can be interpreted as a toxic effect. However, it is more likely that the STZ-related results reflect the real difference between healthy and diabetic animals whereas in the genetic models, the controls already bear some membrane modifications, which are able to cause channel disorders but are not suitable to produce the clinical picture of diabetes.

Diabetes in mice - NIDDM

In the other diabetic model, the amplitudes of the I_{to} in cells from lean mice were similar to that described by Benndorf and Nilius (1988). Nevertheless, the question of the genetically identical control arises also in the case of mice. Phenotypically, all lean animals are similar and they are healthy, they nevertheless represent two different genetic groups, both of which are different from the obese ones. These problems and complications make the interpretation of the data obtained from this particular model difficult as well.

Acknowledgements. The authors are indebted to professor T. Kovács for offering the mice, to dr. B. Nilius for valuable suggestions, and to Ms. Z. Molnár for technical assistance. This work was supported by grants from the Hungarian National Science Foundation (OTKA 1453) and from the Hungarian Ministry of Welfare (ETT T-473/90).

References

Apkon M., Nerbonne J. (1991): Characterization of two distinct depolarization-activated K^+ currents in isolated adult rat ventricular myocytes. J. Gen. Physiol. **97,** 973–1011

Benndorf K., Nilius B. (1988): Properties of an early outward current in single cells of the mouse ventricle. Gen. Physiol. Biophys. **7,** 449–466

Bray G. A., York D. A. (1979): Hypothalamic and genetic obesity in experimental animals: an autonomic and endocrine hypothesis. Physiol. Rev. **59,** 719–809

Butler L., Guberski D. I., Like A. A. (1988): Genetics of diabetes production in the Worcester colony of the BB rat. In: Frontiers in Diabetes Research, Lessons From Animal Diabetes II. (Eds. E. Shafrir and A. E. Renold) pp. 74–78, John Libbey, London

Chappel C. I., Chappel W. R. (1983): The discovery and development of the BB rat colony. An animal model of spontaneous diabetes. Metab. Clin. Exp. **32,** 8–10

Eisenbarth G., Vardi P., Ziegler A., Colman P. G., Nayak R. C., Dotta F., Jackson R. A., Fuji S., Ricker A. T., Rabinowe A., Ikegami H., Soeldner J. S., Hattori M. (1988): Lessons from NOD mouse and BB rat: similarities and contrasts

Escande D., Coulombe A., Faivre J-F., Deroubaix E., Coraboeuf E. (1985): Two types of transient outward currents in adult human atrial cells. Amer. J. Physiol. **249,** H843-H850

Fein F. S., Kornstein L. B., Strobeck J. E., Capasso J. M., Sonnenblick E. H. (1980): Altered myocardial mechanics in diabetic rats. Circ. Res. **47,** 922–933

Fein F. S., Strobeck J. E., Malhotra A., Scheuer J., Sonnenblick E. H. (1981): Reversibility of diabetic cardiomyopathy with insulin in rats. Circ. Res. **49,** 1251–1261

Fein F. S., Aronson R. S., Nordin C., Miller-Green B., Sonnenblick E. H. (1983): Altered myocardial response to ouabain in diabetic rats: mechanics and electrophysiology. J. Mol. Cell. Cardiol. **15,** 769–784

Hamill O. P., Marty A., Neher E., Sakmann B., Sigworth F. J. (1981): Improved patch-clamp techniques for high-resolution current recording from cells and cell-free membrane patches. Pflügers Arch. **391,** 85–100

Hansen A. K. (1989): Principles of breeding, maintaining and working with diabetic and non-diabetic BB/Wor rats. Scand. J. Lab. Anim. Sci. **16,** 15-27

Heidbüchel H., Vereecke J., Carmeliet E. (1990): Three different potassium channels in human atrium. Circ. Res. **66,** 1277–1286

Herberg L., Coleman D. L. (1977): Laboratory animals exhibiting obesity and diabetes syndromes. Metabolism **26,** 59–99

Josephson I. R., Sanchez-Chapula J., Brown A. M. (1984): Early outward current in rat single ventricular cells. Circ. Res. **54,** 157–162

Katz A. M., Messineo F. C. (1981): Lipid-membrane interactions and the pathogenesis of ischemic damage in the myocardium. Circ. Res. **48,** 1–24

Lord J. M., Atkins T. W. (1985): Effect of age on hepatocyte and soleus muscle insulin receptor binding in lean and genetically obese diabetic (ob/ob) mice. Diabetes Res. **2,** 259–265

Magyar J., Rusznák Z., Szentesi P., Szücs G., Kovács L. (1992): Action potentials and potassium currents in rat ventricular muscle during experimental diabetes. J. Mol. Cell. Cardiol. **24,** 841–853

Magyar J., Cseresnyés Z., Rusznák Z., Sipos I., Szüs G., Kovács L. (1995): Effects of insulin on potassium currents of rat ventricular myocytes in streptozotocin diabetes. Gen. Physiol. Biophys. **14,** 191–201

Nagano M., Dhalla N. S. (1992): The Diabetic Heart. Raven Press, New York

Nánási P.P., Varró A., Lathrop D. A. (1992): Ionic currents in ventricular myocytes isolated from the heart of a patient with idiopathic cardiomyopathy. Cardioscience **3,** 85–89

Nobe S., Aomine M., Arita M., Ito S., Takaki R. (1990): Chronic diabetes mellitus prolongs action potential duration of rat ventricular muscles: circumstantial evidence for impaired Ca^{2+} channel. Cardiovasc. Res. **24,** 381–389

Rajatanavin R., Appel M. C., Reinhardt W., Alex S., Yang Y. N., Braverman L. E. (1991): Variable prevalence of lymphocytic thyroiditis among diabetes-prone sublines of BB/Wor rats. Endocrinology **128,** 153–157

Rerup C. C. (1970): Drugs producing diabetes through damage of insulin secreting cells. Pharmacol. Rev. **22,** 485–518

Rodrigues B., McGrath G. M., McNeill J. H. (1989): Cardiac function in spontaneously diabetic BB rats treated with low and high dose insulin. Can. J. Physiol. Pharmacol. **67,** 629–636

Schaible T. F., Malhotra A., Bauman W. A., Scheuer J. (1983): Left ventricular function after chronic insulin treatment in diabetic and normal rats. J. Mol. Cell. Cardiol. **15,** 445–458

Schouten V. J. A. (1984): The relationship between action potential duration and force of contraction in rat myocardium. Eur. Heart. J. **5,** 984–992

Schreiner W., Kramer M., Krischner S., Langsam Y. (1985): Nonlinear least-squares fitting. PC Tech. J. **3,** 170 181

Shibata E. F., Drury T., Refsum H., Aldıete V., Giles W. (1989): Contributions of a transient outward current to repolarization in human atrium. Amer. J. Physiol. **257,** H1773-H1781

Shimoni Y., Banno H., Clack R. B. (1992): Hyperthyroidism selectively modified a transient potassium current in rabbit ventricular and atrial myocytes. J. Physiol. (London) **457,** 369–389

Tomlinson K. C., Gardiner S. M., Hebden R. A., Bennett T. (1992): Functional consequences of Streptozotocin-induced diabetes mellitus, with particular reference to the cardiovascular system. Pharmacol. Rev. **44,** 103–150

Tytgat J., Nilius B., Carmeliet E. (1990): Modulation of the T-type cardiac Ca channel by changes in proton concentration. J. Gen. Phys. **96,** 973–990

Watanabe T., Delbridge L. M., Bustamante J. O., McDonald T. F. (1983): Heterogeneity of the action potential in isolated rat ventricular myocytes and tissue. Circ. Res **52,** 280–290

Westman S. (1968): Development of the obese-hyperglycaemic syndrome in mice. Diabetologia **4,** 141–149

Final version accepted June 15, 1996